Int. Journal of Refractory Metals and Hard Materials 44 (2014) 49–53

Contents lists available at ScienceDirect

Int. Journal of Refractory Metals and Hard Materials

journal homepage: www.elsevier.com/locate/IJRMHM

The effect of HfC content on mechanical properties HfC–W composites

Dongju Lee [a], Malik Adeel Umer [a], Ho J. Ryu [b], Soon H. Hong [a,*]

[a] Department of Materials Science and Engineering, Korea Advanced Institute of Science and Technology, 291 Daehak-ro, Yuseong-gu, Daejeon 305-701, Republic of Korea
[b] Department of Nuclear & Quantum Engineering, Korea Advanced Institute of Science and Technology, 291 Daehak-ro, Yuseong-gu, Daejeon 305-701, Republic of Korea

ARTICLE INFO

Article history:
Received 19 November 2013
Accepted 27 January 2014
Available online 31 January 2014

Keywords:
Composite materials
Powder metallurgy
Sintering
Mechanical properties
Microstructure

ABSTRACT

For improving the mechanical properties of tungsten, HfC–W composites were fabricated by ball milling and spark plasma sintering process. The microstructure and mechanical properties of the composites were investigated. The interdiffusion of the Hf and W atoms during sintering produced a mixed carbide, identified as (Hf,W)C. This interfacial mixed carbide helped in developing a good interface joint with the adjacent W matrix. The increase in mechanical properties of the HfC–W composite at room temperature as well as high temperature was attributed to the reinforcement effect of the HfC particles. One of the strengthening mechanisms of the composite can be attributed to the formation of mixed carbide (Hf,W)C by interdiffusion at the interface, which assured the effective load transfer from the W matrix to the hard HfC particles.

1. Introduction

Due to its high melting point (3440 °C), high modulus of elasticity, thermal shock resistance, and high temperature strength, W and its alloys are often used in high-strength–high-temperature applications [1], such as turbines [2], fusion reactors [3–5], and kinetic energy penetrators [6,7]. One disadvantage of using W is severe oxidation of this material at high temperatures; W loses ~60% of its strength near 1000 °C [8]. Over the past few decades, various materials have been used to enhance the mechanical properties of W at room temperature, as well as at high temperatures. The addition of rhenium (Re) has been shown to increase the room temperature ductility of W, as well as its high-temperature strength [9]. However, Re is expensive and markedly increases the cost of W–Re alloys.

The combination of a refractory metal as the matrix and high-temperature ceramics as the reinforcement has produced composites with an interesting set of chemical, thermal, and mechanical properties. High-temperature ceramics, such as refractory carbides (TiC, Ta_2C, and ZrC), nitrides (TiN and ZrN), and oxides (La_2O_3 and Y_2O_3) have been used to improve the mechanical properties of W through dispersion strengthening at room temperature as well as high-temperature [4,10–13]. However, these materials still experience a significant decrease in their strength at high temperatures probably due to the lower content of ceramic reinforcements (less than 2 wt.%) [14,15]. Therefore, the need for materials having higher temperature capability and higher strength properties, compared with conventional materials, has recently led to the development of high-volume-fraction-reinforced composite materials [16,17]. Among the high-temperature ceramic reinforcements, hafnium carbide (HfC) possesses the highest melting point and superior mechanical properties is considered the most effective second-phase particle for strengthening W at high temperatures. Technological difficulties for obtaining vacuum arc-melted W alloys have shifted the focus to powder metallurgy processes, which are now the primary modes for W matrix composite fabrication. However, to date, there have been no studies on the fabrication of W reinforced with HfC using powder metallurgy.

In this study, we fabricated W matrix composites with a large volume fraction of HfC via the use of spark plasma sintering (SPS). SPS is a process by which powders can be rapidly sintered to full density at relatively low temperatures, compared with conventional sintering processes. The effects of HfC volume fraction on the microstructure and mechanical properties of the composites were studied and compared with monolithic W at room temperature as well as high temperature.

2. Experimental

Tungsten powder (TaeguTec LTD., 2.5 μm, oxygen content: 0.1 wt.%) and HfC powder (LTS Chemical Inc., under 325 mesh (44 μm)) were used to fabricate the W matrix composites. Both powders were dry ball-milled at a rotation speed of 100 rpm using a ball-to-powder ratio of 10:1 for 12 h under Ar. The ball-milling process used 5-mm-diameter tungsten carbide balls. The composite powders were consolidated by SPS (Dr. Sinter Lab. SPS-515S) in a graphite mold at 1800 °C for 3 min with a pressure of 50 MPa under a vacuum of 10 Pa. The heating rate was maintained at 100 °C min^{-1} up to the sintering temperature. For comparison with the composite, monolithic W was prepared using the same conditions. The microstructures of the sintered composites were examined using high-resolution scanning electron microscopy (HR-SEM, Phillips XL30SFEG and FEI NOVA 230) and transmission electron microscopy (TEM, JEOL JEM-2200FS). The composition

* Corresponding author. Tel.: +82 42 350 3327; fax: +82 42 350 3310.
E-mail address: shhong@kaist.ac.kr (S.H. Hong).

0263-4368/$ – see front matter © 2014 Elsevier Ltd. All rights reserved.
http://dx.doi.org/10.1016/j.ijrmhm.2014.01.012

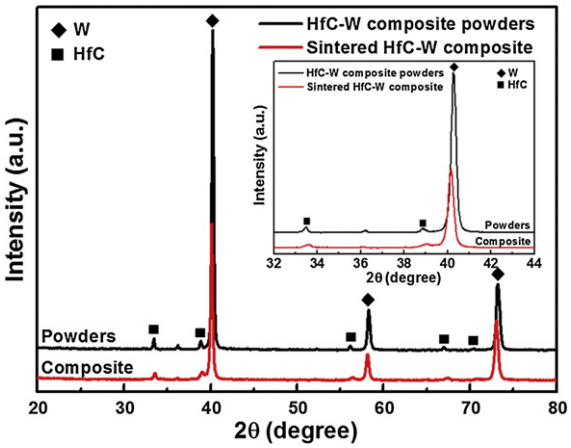

Fig. 1. X-ray diffraction (XRD) patterns of ball-milled HfC–W composite powders and HfC–W composites sintered at 1800 °C. The inset is the enlarged XRD patterns.

and phase analysis were determined by energy-dispersive spectroscopy (EDS) during the TEM process. The grain size of the HfC–W composites was determined using an image analysis program (Matrox Inspector 2). Phase identification of the specimens was performed using X-ray diffraction (XRD, Rigaku D/MAX-IIIC). The relative densities of the composites were measured using the Archimedes' method. The flexural strength of the HfC–W composites was measured using an INSTRON 5583 device with a crosshead speed of 0.2 mm min^{-1} at room temperature. Rectangular composite specimens of $12 \times 1 \times 1.5$ mm, with a span length of 10 mm, were evaluated using the three-point bending test. All surfaces of the specimens were polished using diamond paste, and the edges were chamfered. A computer controlled servo-hydraulic Gleeble 3500 machine was used for the high-temperature compressive strength of the HfC–W composites. Cylindrical compression specimens of 8 mm in diameter and 10 mm in height were machined. Hot compression experiments were conducted under isothermal condition at constant strain rates of 0.1 s^{-1} and at temperatures of 1200 °C under Ar atmosphere. Test specimens were heated to test temperature at the rate of 10 °C/s and soaked for 5 min to secure temperature uniformity prior to deformation. The load-stroke data were converted into true stress–strain curves using standard equations with the elastic deflection of the machine and the grips taken into account. After the measurements, the deformed specimens were quenched in water to freeze the microstructure, sectioned parallel to the compression axis and polished.

3. Results and discussion

XRD patterns of the composite powders and the sintered specimen of 10 vol.% HfC–W composites are shown in Fig. 1. There were only two phases, W and HfC, evident in both the mixed powders and the composites. The peak positions of W and HfC in the XRD patterns of the sintered HfC–W composites were shifted. The diffraction peaks of HfC phases in 10 vol.% HfC–W composites were shifted ~0.2° higher, compared with the peak positions of the HfC powders. The diffraction peaks of the W phases were shifted ~0.12° lower, compared with the peak positions of the W powders (inset of Fig. 1). The XRD results state that there is interdiffusion of W and HfC at the HfC–W interface. We estimate the amount of Hf dissolved in W as well as the amount of W dissolved in HfC. HfC lattice parameter of sintered specimen is

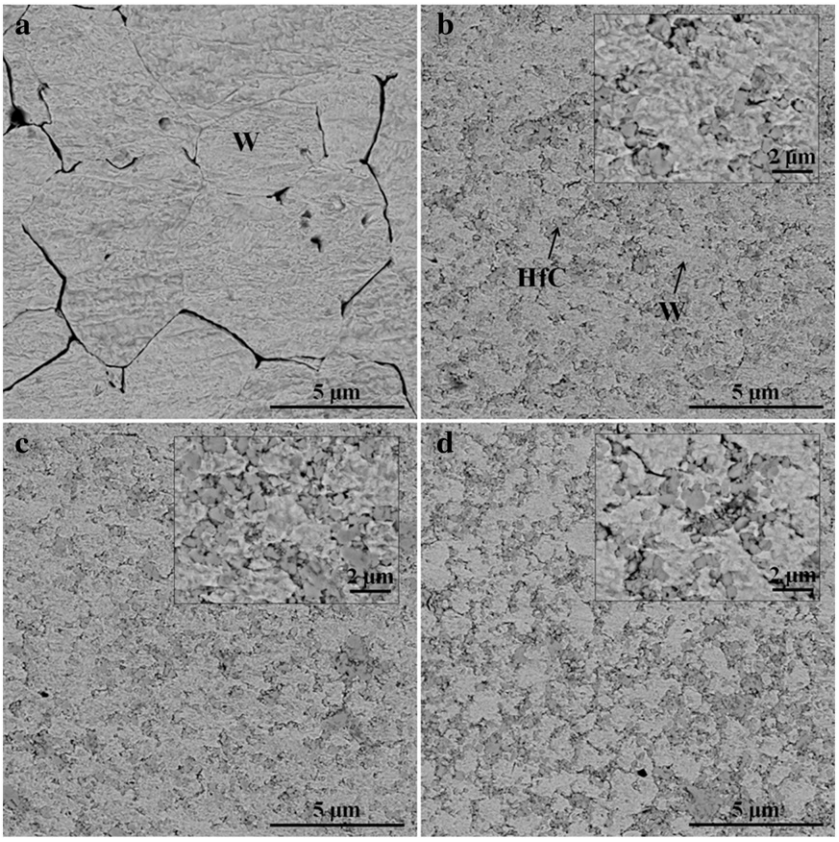

Fig. 2. Microstructure of (a) monolithic W and HfC–W composites with (b) 10 vol.%, (c) 20 vol.%, and (d) 30 vol.% HfC content. All surfaces were polished and etched using Murakami etchant. Insets are higher magnification SEM images.

Table 1
Average grain size of monolithic W and HfC–W composites.

	Average grain size (μm)	Relative density (%)
Pure W	13.8 ± 2.66	99.4 ± 0.4
10 vol.% HfC–W	2.86 ± 0.59	99.3 ± 0.5
20 vol.% HfC–W	2.56 ± 0.57	98.3 ± 0.7
30 vol.% HfC–W	2.27 ± 0.49	96.1 ± 0.6

0.4619 nm compared to 0.4630 nm for as-received HfC powders. Likewire, W lattice parameter of sintered specimen is 0.3174 nm compared to 0.3165 nm for as-received W powders. As a result, the amount of Hf dissolved in W is about 2.5 at.% as well as the amount of W dissolved in HfC is 3.1 at.%. Lattice parameter change according to carbon content is negligible over 49.5 at.% of carbon content (lattice parameter 0.4636 nm). [18–20].

The microstructures of HfC–W composites consolidated with different HfC volume fractions are shown in Fig. 2a–d. The surfaces of HfC–W composites were etched with Murakami etchant. In the SEM images, the dark gray phase was identified as HfC; the light gray phase corresponded to W. The HfC particles were observed to be homogeneously distributed in the W matrix. The uniformity of the microstructure was expected to instill isotropic physical properties in the HfC–W composites. The average grain size of the HfC–W composites was significantly smaller than that of monolithic W, as listed in Table 1. This implies that HfC inhibits the grain growth of W during the sintering process. Smaller W grains are useful for improving the strength and toughness of the HfC–W composite [21]. Also, the relative density decreased and the agglomeration of HfC particles increased with increasing HfC volume fraction.

A small number of tiny pores were present within some of the HfC particle clusters, due to poor sinterability between the HfC particles. These tiny pores, located between the HfC particle clusters, can become latent sources for microcrack formation. There was no evidence of pores in the W matrix or at the HfC–W interface. The agglomeration and HfC–HfC particle interaction increased with the volume fraction of HfC in the W matrix.

The morphology and interface between W and HfC phases were examined by TEM, as shown in Fig. 3a–d. Fig. 3a shows low-magnification TEM images indicating the interface of W and HfC. The bright and dark phases corresponded to HfC and W, respectively, as identified by EDS. Fig. 3b shows an HR-TEM image of the direct contact between W and HfC at the interface. The W region displays the crystallographic (110) plane, which has a BCC crystal structure and *d*-spacing of 0.22 nm; the HfC region indicates a crystallographic (111) plane, which has a cubic crystal structure and a *d*-spacing of 0.266 nm. The insets of Fig. 3b show fast-Fourier transform (FFT) images of the HR-TEM images. HAADF-STEM image and EDS mapping of the HfC–W interfacial region indicate that there is interdiffusion of W and Hf at the HfC–W interface, as shown in Fig. 3c–d. In order to distinguish between an only hafnium-enriched zone in the W matrix or a mixed carbide (Hf,W)C, an EDS line scan was conducted, as shown in Fig. 4. In this case, Hf and C atoms

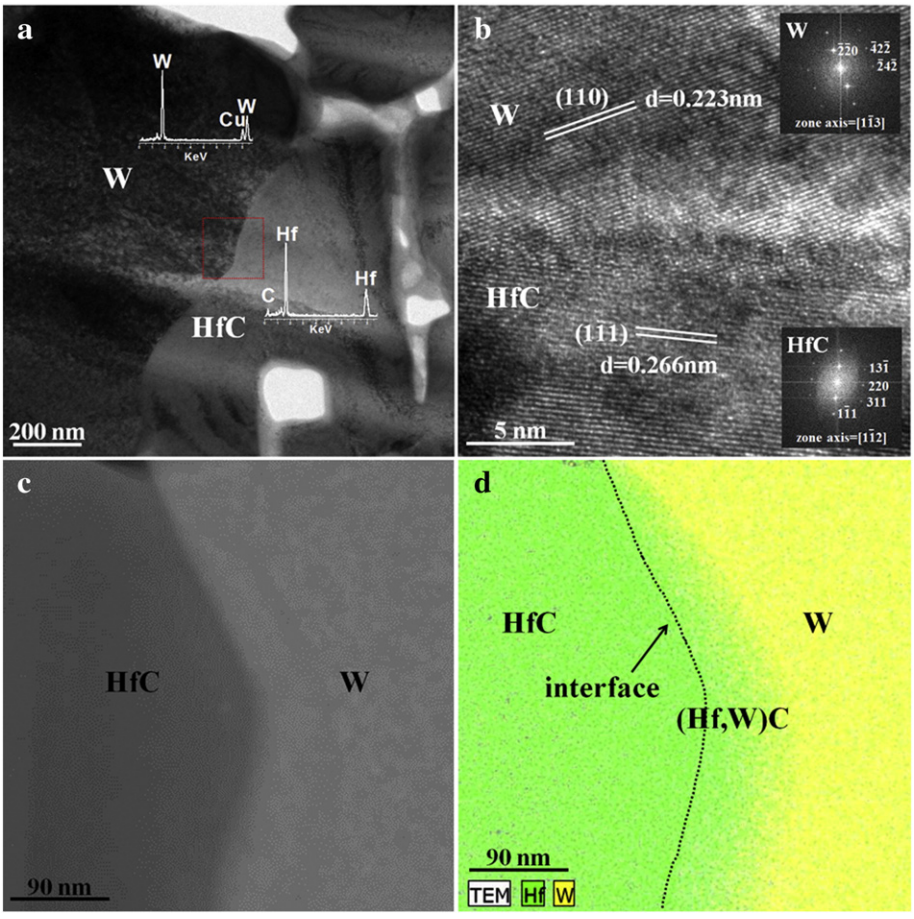

Fig. 3. Transmission electron microscopy (TEM) images of the 10 vol.% HfC–W composite. (a) Low-magnification TEM image showing a clean HfC–W interface and no other phases or interfacial precipitates. (b) High-resolution TEM (HR-TEM) image of the interface and corresponding fast-Fourier transform (FFT) images. (c) HAADF-STEM image of the interface tilted at an angle of 15°. (d) Energy dispersive spectroscopy (EDS) mappings of the HfC–W interfacial region showing interdiffusion at the HfC–W interface. (Note: Since the journal is printed in black and white only the readers are advised to visit the internet version of this paper where color is retained for a better study of the element distribution).

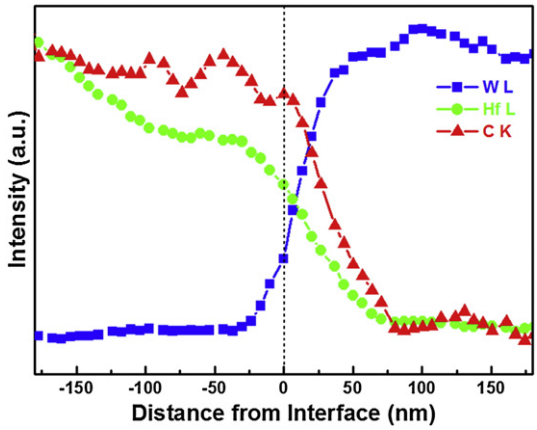

Fig. 4. Energy dispersive spectroscopy (EDS) line scan of tungsten (W), hafnium (Hf), and carbon (C) at the HfC–W interface as a function of the distance from the interface.

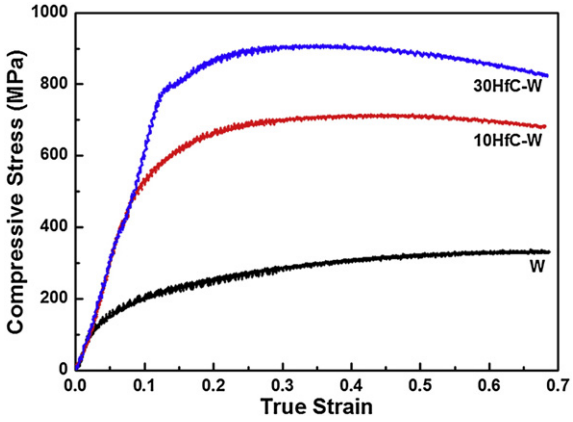

Fig. 6. High temperature compressive stress–strain curve of the HfC–W composites with HfC content at 1200 °C.

penetrated into the W grains as the temperature approached the sintering temperature; this led to the formation of mixed carbide, identified as (Hf,W)C. The formation of mixed carbide (Hf,W)C may be beneficial for strengthening HfC–W composites. [21,22].

Fig. 5a shows the flexural strength and compressive strength of the HfC–W composite and monolithic W at room temperature. The flexural strength and compressive strength increased with the addition of HfC particles. The HfC particles present in the W matrix effectively constrained plastic deformation of the W matrix by hindering dislocation motion, thereby enhancing the strength of the HfC–W composite. [11] The flexural strength of the composites increased with increasing HfC content, reaching a maximum value of 1578 MPa at 10 vol.% HfC; the composite strength began to decrease as the HfC content increased further. In contrast, the compressive strength of the composites increased with an increase in the HfC content. This behavior was completely analogous to the microstructure of the composites. The highest value of the flexural strength was obtained for samples that possessed a uniform microstructure with the lowest degree of agglomeration [23]. Since the flexural strength is more sensitive to agglomeration and inhomogeneities in the microstructure than the compressive strength, a decline in the values of flexural strength occurs, contrary to a rise in compressive strength [3].

A high-temperature compression test was carried out at a temperature of 1200 °C to examine the high-temperature deformation behavior of HfC–W composite. As shown in Fig. 6, a high-temperature compression strength of the composites gradually increased with an increase in proportion to the added amount of HfC. This means that the dispersion strengthening of the HfC particles stable at high temperatures inhibits the deformation of the composites and that the addition of the HfC particles effectively enhances the high-temperature compression strength.

Fig. 7 shows SEM images of the fracture surfaces of monolithic W and HfC–W composites. The fracture surface of W exhibited a typical brittle fracture consisting of a dominant intergranular fracture (Fig. 7a). In pure W, the grain boundary is relative weak, compared with the W grain itself. In contrast, 10 vol.% HfC–W composites showed a transgranular fracture with a river pattern, as shown in Fig. 7b. With the addition of HfC particles, the dominant fracture converted from an intergranular mode to a transgranular mode; this indicated an increase in the flexural strength of the composites by the mixed carbide (Hf,W)C formed by interdiffusion at the interface. Additionally, the strengthening particles with high hardness will deflect the crack propagation path and make it flexuous. A more flexuous crack propagation path will consume more crack propagation energy, which leads to greater fracture toughness [21]. However, large HfC particle clusters prefer an intergranular fracture at the interface between HfC and HfC particles (Fig. 7c–d). For 20 and 30 vol.% HfC–W composites, many pores were found in the large HfC particle clusters; these pores will become fracture sources under loading. Therefore, the intergranular fracture mode and the pores in the large HfC particle clusters for the composites could lead to low composite strengths for composites with a high volume fraction of HfC particles [22].

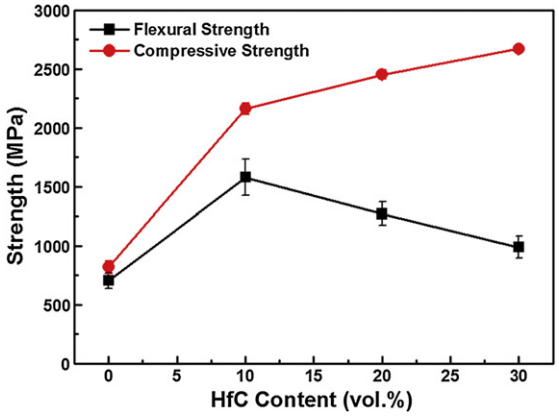

Fig. 5. Flexural strength and compressive strength of the HfC–W composites as a function of HfC content at room temperature.

4. Conclusion

The addition of HfC particles into the W matrix had beneficial effects on the mechanical properties of the composites. As Hf and W atoms interdiffuse at the sintering temperature, a mixed carbide, identified as (Hf,W)C, was formed. The formation of such mixed carbide may be beneficial for strengthening HfC–W composites by forming strong interfacial bonds for effective load transfer to the HfC particles. Moreover, the HfC particles dispersed at the W grain boundaries inhibited the growth of W grains during the sintering process, enhancing the mechanical properties of the composite.

Acknowledgments

This research was supported by NSL (National Space Lab.) program through the Korea Science and Engineering Foundation (NRF-2008-2003213) and Priority Research Centers Program through the National Research Foundation of Korea (NRF) funded by the Ministry of Education, Science and Technology (2011-0031407).

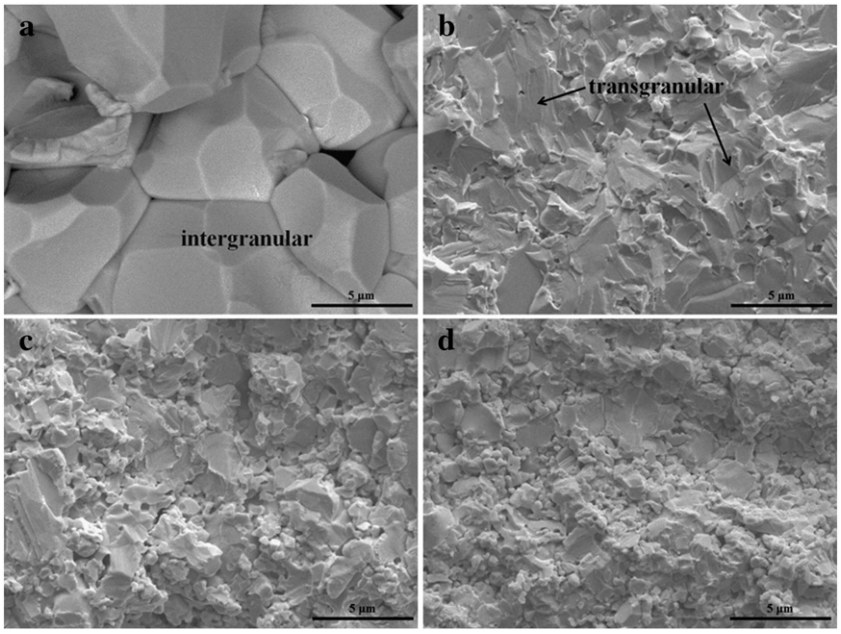

Fig. 7. Scanning electron microscopy (SEM) images of the fracture surfaces of (a) monolithic W and HfC–W composites with (b) 10 vol.%, (c) 20 vol.%, and (d) 30 vol.% HfC content.

References

[1] Lassner E, Schubert W-D. Tungsten: properties, chemistry, technology of the element, alloys, and chemical compounds. New York: Kluwer Academic/Plenum Publishers; 1999.

[2] Mabuchi M, Okamoto K, Saito N, Asahina T, Igarashi T. Deformation behavior and strengthening mechanisms at intermediate temperatures in W–La_2O_3. Mater Sci Eng A 1997;237:241–9.

[3] Lee D, Umer MA, Shin Y, Jeon S, Hong S. The effect of sintering conditions and ZrN volume fraction on the mechanical properties of spark plasma sintered W/ZrN composites. Mater Sci Eng A 2012;552:481–5.

[4] Chen Y, Wu YC, Yu FW, Chen JL. Microstructure and mechanical properties of tungsten composites co-strengthened by dispersed TiC and La_2O_3 particles. Int J Refract Met Hard Mater 2008;26:525–9.

[5] Wang YJ, Peng HX, Zhou Y, Song GM. Influence of ZrC content on the elevated temperature tensile properties of ZrCp/W composites. Mater Sci Eng A 2011;528:1805–11.

[6] Upadhyaya A. Processing strategy for consolidating tungsten heavy alloys for ordnance applications. Mater Chem Phys 2001;67:101–10.

[7] Magness LS. High-strain rate deformation behaviors of kinetic-energy penetrator materials during ballistic impact. Mech Mater 1994;17:147–54.

[8] Yih SWH, Wang CT. Tungsten: sources, metallurgy, properties, and applications. New York: Plenum Press; 1979.

[9] Roosta M, Baharvandi H, Abdizade H. The evaluation of W/ZrC composite fabricated through reaction sintering of two precursors: conventional ZrO_2/WC and novel $ZrSiO_4$/WC. Int J Refract Met Hard Mater 2011;29:710–5.

[10] Roosta M, Baharvandi H. The comparison of W/Cu and W/ZrC composites fabricated through hot-press. Int J Refract Met Hard Mater 2010;28:587–92.

[11] Teague MC, Hilmas GE, Fahrenholtz WG. Reaction processing of ultra-high temperature W/Ta2C-based cermets. J Am Ceram Soc 2009;92:1966–71.

[12] Zhang TQ, Wang YJ, Zhou Y, Song GM. High temperature electrical resistivities of ZrC particle-reinforced tungsten-matrix composites. Int J Refract Met Hard Mater 2010;28:498–502.

[13] Chen ZC, Zhou ML, Zuo TY. Morphological evolution of second-phase particles during thermomechanical processing of W–La_2O_3 alloy. Scr Mater 2000;43:291–7.

[14] Luo A, Shin KS, Jacobson DL. Hafnium carbide strengthening in a tungsten rhenium matrix at ultrahigh temperatures. Acta Metall Mater 1992;40:2225–32.

[15] Luo A, Jacobson DL, Shin KS. Tensile properties of tungsten 3.6-percent rhenium 0.4-percent hafnium carbide above 0.5 Tm. Scr Metall Mater 1989;23:397–400.

[16] Song GM, Wang YJ, Zhou Y. Elevated temperature ablation resistance and thermophysical properties of tungsten matrix composites reinforced with ZrC particles. J Mater Sci 2001;36:4625–31.

[17] Song GM, Zhou Y, Wang YJ. Effect of carbide particles on the ablation properties of tungsten composites. Mater Charact 2003;50:293–303.

[18] Rudy E. Compendium of phase diagram data. Air Force Materials Lab., Wright-Patterson AFB, OH; 1969 102 [Report No. AFML-TR-65–2].

[19] Artyukh LV, Velikanova TY, Eremenko VN. Physicochemical interaction of tungsten carbides with hafnium carbide. Inorg Mater 1979;15:497–500.

[20] Nowotny H, Kieffer R, Benesovsw F, Brukl C, Ruby E. The partial systems of HfC with TiC, ZrC, VC, NbC, TaC, Cr_3C_2, Mo_2C (MoC), WC and UC. Monatsh Chem 1959;90:669–79.

[21] Song GM, Wang YJ, Zhou Y. The mechanical and thermophysical properties of ZrC/W composites at elevated temperature. Mater Sci Eng A 2002;334:223–32.

[22] Song GM, Wang YJ, Zhou Y. Thermomechanical properties of TiC particle-reinforced tungsten composites for high temperature applications. Int J Refract Met Hard Mater 2003;21:1–12.

[23] Mukhopadhyay AK, Datta SK, Chakraborty D. Fracture toughness of structural ceramics. Ceram Int 1999;25:447–54.